Friction and work function oscillatory behavior for an even and odd number of layers in polycrystalline MoS₂

Francesco Lavini,[1,2,3] Annalisa Calò,[1,3] Yang Gao,a Edoardo Albisetti,[1,4] Tai-De Li,[1] Tengfei Cao,[2,5] Guoqing Li,[6] Linyou Cao,[6,7] Carmela Aruta*,[8] and Elisa Riedo*,[1,2,3,9]

* E-mail: elisa.riedo@nyu.edu, carmela.aruta@spin.cnr.it

[1] Advanced Science Research Center, City University of New York, NY 10031, USA.

[2] CUNY Graduate Center, Ph.D. Program in Physics and Chemistry, NY 10016, USA

[3] Tandon School of Engineering, New York, USA

[4] Dipartimento di Fisica, Politecnico di Milano, 20133 Milano, Italy

[5] Department of Chemistry, College of Staten Island, City University of New York, New York 10314, USA

[6] Department of Materials Science and Engineering, North Carolina State University, Raleigh, USA

[7] Department of Physics, North Carolina State University, Raleigh, NC 27695, USA

[8] National Research Council CNR-SPIN, I-00133 Rome, Italy

[9] Physics Department, City College of New York, City University of New York, Marshak Science Building, New York 10031, USA

ABSTRACT

The ability to understand the relationship between friction, adhesion, electric charges and defects two-dimensional (2D) materials is of key importance for their assembly and use in nano-electro-mechanical and energy harvesting systems. Here, we report on a new oscillatory behavior of nanoscopic friction in continuous polycrystalline MoS₂ films for an odd and even number of atomic layers, where odd layers show higher friction and lower work function. Friction force microscopy combined with Kelvin probe force microscopy and X-ray photoelectron spectroscopy demonstrates that an enhanced adsorption of charges and OH molecules is at the origin of the observed increase in friction for 1 and 3 polycrystalline MoS₂ layers. In polycrystalline films with an odd number of layers, each crystalline nano-grain carries a dipole due to the MoS₂ piezoelectricity, therefore charged molecules adsorb at the grain boundaries all over the surface of the continuous MoS₂ film. Their displacement during the sliding of a nano-size tip gives rise to the observed enhanced dissipation and larger nanoscale friction for odd layer-numbers. Similarly, charged adsorbed molecules are responsible for the work function decrease in odd layer-number.

INTRODUCTION

Nanoscopic manipulation, control and investigation of atomically thin sheets of a variety of 2D materials[1,2] from graphene[3,4] to transition metal dichalcogenides (TMDC), such as MoS₂,[5–7] has opened the route for observing and understanding new fascinating physical properties, and for their practical use in several device technologies.[8–10] 2D materials also offer the opportunity to shed light on the molecular mechanisms underlying friction,[11–18] one of the oldest, complex and still pressing problems in a variety of industrial applications today, from the automotive/transportation industry to microelectromechanical systems (MEMS). Beside the fundamental scientific interest, 2D materials and in particular MoS₂ have many potential applications in nanoelectromechanical systems (NEMS),[12,19,20] lubrication, energy harvesting,[21,22] and flexible electronic devices.[10] For all these applications, it is very important to comprehend the tribological behavior of MoS₂ when reduced to

the 2D thin film scale. A characteristic unique frictional behavior has been recently found in 2D exfoliated single crystal flakes of MoS_2, where friction forces decrease when increasing the number of atomic layers, approaching the value of the bulk case.[13] This behavior was believed to be universal for 2D materials and was explained as due to a puckering effect, where adhesion to a sliding probe creates out-of-plane deformations of thinner sheets, leading to an increased contact area and, hence, friction. Nevertheless, it remains unclear if the same model applies for extended continuous polycrystalline 2D films, grown for example by chemical vapor deposition (CVD), which are very attractive for large scale industrial applications and MEMS fabrication.[23]

Here we show for polycrystalline MoS_2 an oscillatory behavior with higher friction for an odd number of layers and lower friction for an even number of layers. We perform atomic force microscopy (AFM) based friction force microscopy (FFM) measurements at different humidity, combined with Kelvin probe force microscopy (KPFM) and X-ray photoelectron spectroscopy (XPS) and we demonstrate that an enhanced adsorption of charges and charged molecules all over the surface of polycrystalline MoS_2 films with an odd number of layers is at the origin of the observed increase in friction for 1 and 3 layers (1L, 3L) under ambient conditions. In particular, XPS demonstrates an enhanced adsorption of hydroxyl species at the surface of polycrystalline MoS_2 films containing an odd number of layers, a fact that shifts the Fermi energy towards the conduction band, lowering the work function of the odd layers, as determined by KPFM. It is well known in the literature[21,22] that single crystal MoS_2 flakes with an odd number of layers are piezoelectric with a net in-plane polarization that can be neutralized by free charges or molecules adsorbed at the edges of the flakes. On the other hand, in a polycrystalline film with an odd number of layers, each nano-crystalline grain carries a dipole that attracts charges and charged molecules at the grain boundaries (GB) present all over the surface (see Fig. 1). These charges and charged molecules, present only on the surface of 1L and 3L polycrystalline MoS_2 samples, are displaced during the sliding of the AFM tip on the MoS_2 surface in friction experiments, giving rise to an enhanced dissipation and larger frictional forces in an odd number of layers.

Friction at the micro- and nanoscale in a FFM experiment is dominated by short-range interactions between the sliding tip and the surface. Indeed, being an energy-dissipating process, it strongly depends on the potential energy landscape of the tip–surface interactions,[24,25] and the literature shows several examples of the key role of charges and electronic dissipation in sliding friction.[26,27] This oscillatory friction behavior is not present in the large micron-size single crystal MoS_2 triangular flakes containing 1 or 3 layers, where charges are present only at the crystal edges, which are several micrometers apart, having a negligible impact on nanoscale friction.

EXPERIMENTAL SECTION

CVD polycrystalline and single crystal MoS2 films

Growing uniform and continuous MoS_2 thin films over large areas, additionally controlling the number of layers, is challenging because MoS_2 monolayers coexist with by-products with a higher thickness. In this work continuous polycrystalline 1 cm^2 MoS_2 films are used, which are produced following a recently developed approach.[5] In our study, we analyze four types of polycrystalline MoS_2 films with a defined thickness, from 1 to 4 atomic layers.

Crystalline quality and thickness are characterized by AFM, STEM and Raman spectroscopy (see Supporting Information, Fig. S1–S3). For comparison, we also investigate MoS2 single crystals of ~1 μm size, also grown by CVD on sapphire according to a reported procedure.[28–30] Using MoO_3 together with S powders as precursors allows the growth of MoS_2 single crystals with characteristic

triangular shapes. In particular, the excess of Mo precursor enhances the vertical growth, with thicknesses progressively ranging from one to several atomic layers (10L).

Friction force microscopy

Friction force microscopy measurements, together with topography imaging, are performed in contact mode with a Bruker Multimode 8 AFM. We use silicon AFM probes (PPP-CONT Nanosensor) with a normal spring constant k between 0.2–0.4 N m^{-1}, calibrated using the thermal noise method.[31] The lateral spring constant is obtained from the normal one using a conventional relationship for a rectangular cantilever[32] (more details are reported in the Supporting Information). We underline that, although the spring constant is carefully calibrated, small changes in the tip size may vary the absolute value of the measured friction forces. For this reason, freshly cleaved bulk MoS_2 is measured at the beginning and at the end of each set of experiments as a reference for the absolute values of friction, to ensure reliability in the comparison between samples at different numbers of layers. Our experiments are performed on three batches of polycrystalline MoS_2 films, where each batch includes four films, with atomic thicknesses of 1, 2, 3, and 4 layers, along with several different single crystal MoS_2 structures with the same thickness. During each series of friction measurement, we scan each sample over a 1×0.5 μm^2 area, with a scanning speed of 2 μm s^{-1} (1 Hz), collecting data at different normal loads, from 3 nN to 18 nN, on multiple positions of each sample. Each reported friction data point per load and per individual sample (i.e. polycrystalline or single crystal, with a given number of layers) therefore represents the average value over 9 different series and forty different measurements. Finally, each complete series of friction experiments, comparing 1L to 4L polycrystalline films and single crystals, as well as bulk MoS_2, under humid and dry conditions is usually performed within the same day to ensure the same conditions for the tip and environment. After collecting friction scans in a humid environment (RH = 45 ± 5%), at 15 nN normal load, we bring the scanning environment to low relative humidity (RH ≈ 5%), and perform an entire set of friction force measurement. This procedure is standardized for all samples. If the friction measurements on the reference MoS_2 bulk sample suggest that the tip has changed properties or has been damaged, the whole set of experiments is discarded.

During friction measurements performed under humid conditions, relative humidity (RH) is constantly monitored to be 45 ± 5%. For measurements under dry conditions, RH is kept around 5% by using an AFM fluid cell and flowing nitrogen gas (N_2) in it for 15 minutes, and let the environment in the cell rest for other 5/10 minutes, to stabilize the measurement system. Before conducting the experiments under dry conditions, we perform some scans under humid conditions for each sample, within the same range of normal loads. In this way, it is possible to observe directly the variation of friction forces with relative humidity.

X-Ray photoelectron spectroscopy (XPS)

X-ray photoelectron spectroscopy (XPS) measurements are used to analyze the chemical configuration of the samples, including their valence states. Measurements are performed with the Physical Electronics VersaProbe II using Al Kα radiation (1486.6 eV). We collect Mo 3d, S 2p, and O 1s core level spectra for all polycrystalline samples, from 1L to 4L, to study the influence of thickness on the binding energies and composition. We also measure the valence band spectra by finely scanning close to the Fermi edge, where the binding energy is zero. More details about the measurements and the fitting procedure are provided in the Supporting Information (Fig. S4–S6). As mentioned above, the characteristic dimension of the MoS_2 single crystals used in our study is about 1 μm, and the distribution and density of the crystals on the surface is such that crystals of different, random thicknesses can be found within the same micrometer-size area (see Fig. S2c–e of the Supporting Information). Since the lateral spatial resolution used during the XPS experiments is about

200 μm, it is impossible to isolate crystals with only one population of thickness. Mo 3d and S 2p core level spectra, resulting from the contributions of single crystals with different thicknesses, are reported in the Supporting Information in Fig. S4.

Kelvin probe force microscopy (KPFM)

Frequency-modulated Kelvin Probe Force Microscopy (FM-KPFM) experiments are performed with the same Bruker Multimode 8 AFM used for friction measurements and using Pt/Ir coated cantilevers with a resonance frequency f ∼ 75 kHz and a spring constant 0.5–10 N m^{-1} (PPP-EFM Nanosensors). Polycrystalline and single crystal CVD MoS_2 samples (size =0.5 × 0.5 cm^2) are glued on metallic sample holder disks with conductive tape and then additionally connected to the sample holders with silver paste. Topography and KPFM images (2 × 2 μm^2, 512 × 512 pixels) are collected at a scan rate of 0.2 Hz for polycrystalline MoS_2 samples, while 256 × 256 pixel images are collected at a scan rate of 1 Hz for single crystal MoS_2 samples. The amplitude of the AC voltage used for FM-KPFM measurements is set at 4 V in order to ensure low-noise FM-KPFM images while avoiding artifacts in the AFM topography. The work function (WF) of MoS_2 samples is obtained from contact potential difference (CPD) images according to the following equation: $W_F^{MoS2} = W_F^{tip} + e \cdot CPD$, where e is the electronic charge and W_F^{tip} is extracted from the CPD images of a gold calibration sample, assuming $W_F^{gold} = 5.1$ V (ref. 33 and 34) (see Fig. S9 of the Supporting Information). For the polycrystalline samples, W_F^{MoS2} (average value and standard deviation) is obtained from a Gaussian fit of the normalized distribution histogram from the KPFM images shown in Fig. 4d and S7 of the Supporting Information. Each histogram shows the number density of pixels at each W_F *vs.* the corresponding W_F. For single crystal samples, W_F^{MoS2} F (average value and standard deviation) is obtained from the average and RMS values of CPD taken on rectangular areas inside each crystal of a certain thickness, from 1L to 10L (KPFM images are shown in Fig. S8b and d of the Supporting Information).

RESULTS AND DISCUSSION

In the present study, we use atomic force microscopy (AFM) to explore the friction behavior of continuous polycrystalline films of MoS_2 (Fig. 1a), which are grown by CVD on sapphire5 (see also the Experimental section and the Supporting Information). $MoCl_5$ and sulfur powder are used as precursors to obtain a self-limiting deposition with a superficial, rather than vertical growth, leading to large area (1 × 1 cm^2), atomically thin polycrystalline samples of uniform thickness. These MoS_2 films contain crystalline grains varying from tens to hundreds of nanometers, which are observable in AFM and in transmission electron microscopy (TEM) images (Fig. 1a and d).
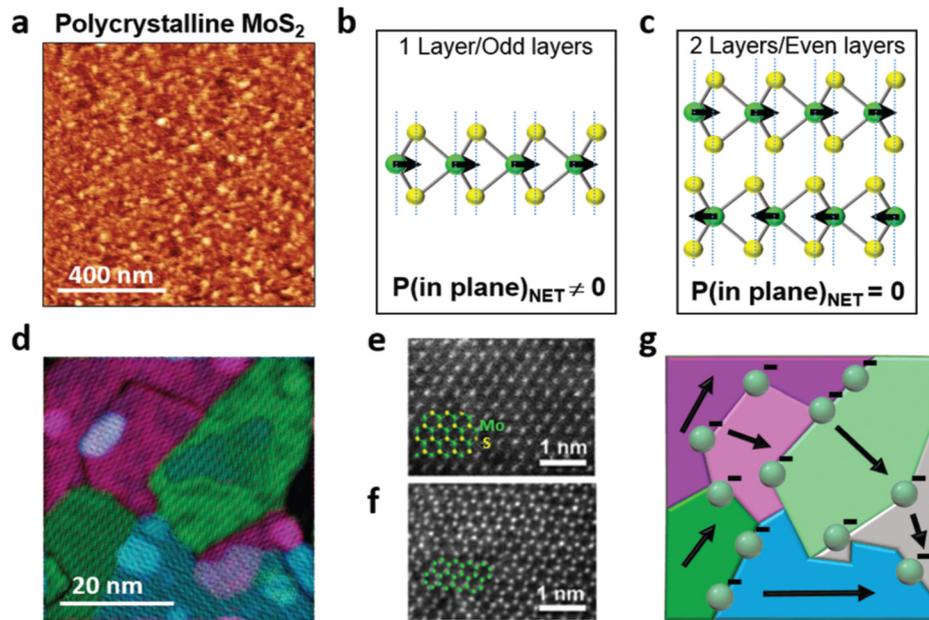
Fig. 1 Schematic representation, TEM, STEM and AFM topography of CVD polycrystalline MoS_2.

In our study, we analyze polycrystalline MoS_2 samples with four different thicknesses, namely 1, 2, 3, and 4 atomic layers. Vertical alignment of the layers is explored via scanning transmission electron microscopy (STEM). High-angle annular dark field (HAADF) images of MoS_2 mono- and bilayer films (Fig. 1e and f, respectively) show a substantial difference in their lattice orientation, indicating an AB stacking sequence in the bilayer, where Mo atoms of the top layer overlap with the sites of S atoms in the underlying layer. Because of its crystal structure, a single layer of MoS_2 shows a broken inversion symmetry associated with a net in-plane permanent polarization (see Fig. 1b),[21] while no net in-plane permanent polarization is present in the symmetric even numbered layers, e.g. 2, 4 layers (Fig. 1c).

Therefore the layer alignment inside each grain very likely gives rise to a net in-plane dipole in each grain in odd numbered layers, and its disappearance for even-numbered layers. Samples are characterized by AFM topography, Raman spectroscopy and electron microscopy, as reported in the Supporting Information (Fig. S1–S3).

For comparison, we also investigate MoS_2 single crystals with characteristic triangular shapes of micrometer size, also grown by CVD on sapphire.[28–30] In particular, the excess of Mo precursor in this method enhances the vertical growth of each single crystal, with thicknesses progressively ranging from one to several atomic layers (10L). Thus, these MoS_2 structures also exhibit 1L, 2L, 3L, and 4L crystals of a few micrometers that can be easily distinguished in AFM images and serve as a comparison with polycrystalline samples. An AFM image of a 1L MoS_2 single crystal is shown in the inset of Fig. 2b.
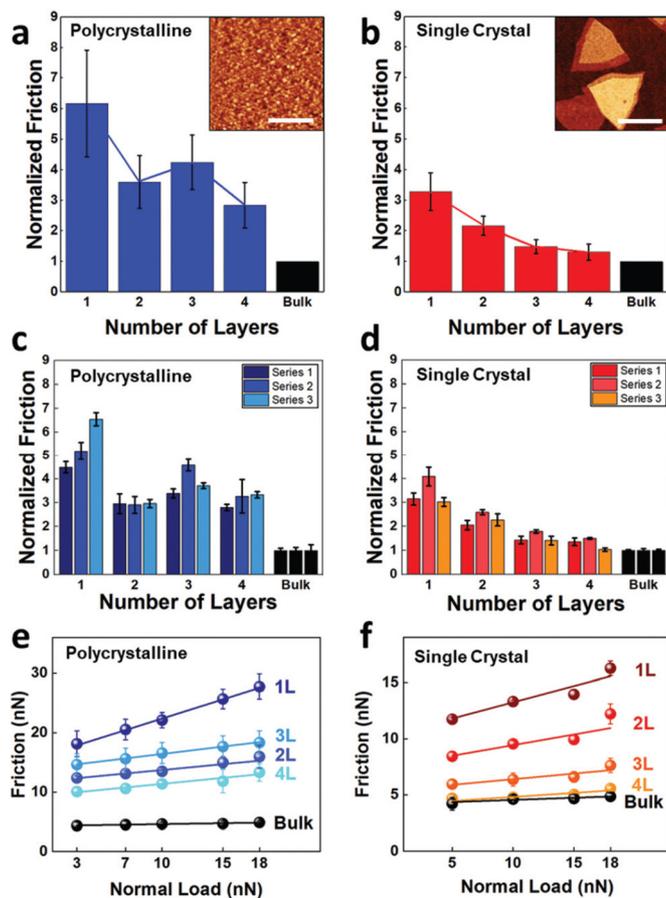
Fig. 2 Friction of single crystal and polycrystalline CVD MoS$_2$ under humid conditions.

Fig. 2a and b show the average friction force as a function of the number of atomic layers, obtained from FFM experiments performed in a humid environment (relative humidity RH = 45%) on polycrystalline MoS$_2$ films and on MoS$_2$ single crystals respectively. The friction values are extracted from $1 \times 0.5 \ \mu m^2$ area friction images and averaged over more than 40 measurements for each load and sample, see the Experimental section for more details. Graphs are obtained normalizing the friction values of the different samples with the ones obtained for freshly cleaved bulk MoS$_2$. Fig. 2a and b clearly show a different behavior between MoS$_2$ polycrystalline films and single crystals, as friction forces under ambient conditions are significantly larger for the former compared to the latter. Furthermore, very interestingly, while friction on single crystal MoS$_2$ monotonically decreases as a function of thickness, as previously observed in the literature for single crystal MoS$_2$ flakes,[13] on polycrystalline films we observe an oscillatory behavior with higher friction forces for 1L and 3L (odd numbered layers) and smaller friction forces for 2L and 4L (even-numbered layers). This oscillation is superimposed to a monotonic downward trend towards the bulk value.

We remark that in Fig. 2a we show the average friction force values obtained from 9 different series of experiments on polycrystalline MoS$_2$ films with four different thicknesses, for a total of 36 series, and each of these 9 series includes friction experiments for films with 1, 2, 3, 4 layers, where these four films for each series are previously grown in the same 24–48 hours' time-window. Specifically, three different "batches" of samples have been investigated, such that we performed 4 series of experiments on batch #1 (1, 2, 3, 4L), 3 series on batch #2 (1, 2, 3, 4L) and 2 series on batch #3 (1, 2, 3, 4L).

Furthermore, each series of friction experiments includes several measurements in different regions of the surface for each number of layers and each series follows a given random sequence in terms of

the order in which the samples are measured. Because we measure three different batches of samples, and 9 different series over a period of one year, the friction standard deviation for each thickness displayed in Fig. 2a and calculated over all the measurements (~40 for each thickness) is quite large; however it is important to underline that the oscillatory friction behavior is present for each of the three batches of samples, and more generally for each of the 9 series. For example, we show in Fig. 2c the normalized friction force values from 3 different series, each corresponding to one of the 3-different batches of samples, showing a clear oscillatory friction behavior with the number of layers. The relative error bar shown in this figure corresponds to the deviation of friction values within different regions of the same sample. It is thus clear how the oscillatory behavior is a property of polycrystalline MoS_2 and does not depend on the conditions of the single experiment or on the batch of samples used. For comparison, we also show three different series of measurements on single crystal MoS_2 samples in Fig. 2d.

The observed variation of the friction force with the number of layers in polycrystalline MoS_2 films can have different explanations. The friction force (F_F) at the nanoscale is related to the friction coefficient (μ), the adhesion force (F_{adh}) and the normal forces (F_N). In the first approximation and in the range of loads we are considering, F_F is given by the following equation:[18,35]

$$F_F = \mu(F_N + F_{adh}) \tag{1}$$

To understand the origin of the observed friction oscillations in polycrystalline MoS_2 films, we measure the friction forces as a function of the normal applied load for each sample at the same RH = 45%. The results are shown in Fig. 2e. For comparison, the same measurements are also performed on single crystal MoS2 triangular structures, under the same conditions (see Fig. 2f). The friction data for each type of sample are fitted with a linear fit, according to Eqn 1. The extracted μ and F_{adh} values are reported in Table 1 and in Table S3 of the Supporting Information, respectively.

	Polycrystalline μ	Single crystal μ
1L	0.65 ± 0.03	0.29 ± 0.05
2L	0.20 ± 0.02	0.19 ± 0.06
3L	0.25 ± 0.01	0.10 ± 0.03
4L	0.18 ± 0.02	0.07 ± 0.02
Bulk	0.04 ± 0.01	0.04 ± 0.01

Table 1 Friction coefficient μ, and the corresponding standard deviation for MoS_2 samples

The fitting procedure shows that for MoS_2 single crystals the friction coefficient monotonically decreases when increasing the thickness, approaching the low values of the bulk MoS_2 for L > 4. This decrease is in agreement with previous results on MoS_2 single crystal flakes.[13] It was also previously shown that for exfoliated single crystal MoS_2 the adhesion force does not critically change with atomic thickness,[13] and this result is in agreement with our findings for single crystal MoS_2 (see Table S3 of the Supporting Information, right column). On the other hand, for the polycrystalline films, friction coefficients are higher for 1L and 3L compared to 2L and 4L (see Table 1), showing that superimposed to the previously observed monotonic downward trend towards the bulk value, we observe an oscillatory behavior between odd and even numbers of layers. Regarding the adhesion forces, we did not observe any clear dependence of the measured F_{adh} on the number of layers for polycrystalline MoS_2 samples. Thus, adhesion seems to be unrelated to the observed oscillatory trend of F_F in polycrystalline MoS_2. For polycrystalline samples (Table S3 of Supporting Information, left column), we notice that the 1L sample displays a significantly lower value of adhesion force compared to the thicker samples. It may be possible that in this case a high density of negatively

charged particles concentrated on the film surface (see further in the text) changes the contact between the tip and surface through the effect of electrostatic forces. Indeed, it has been observed that adhesion force decreases with increasing concentration of OH− on the surface of metals and semiconductors, generating a repulsive component that directly affects the tip contact.[36] We also fit the friction data accordingly with the single-asperity 2/3 power law equation[37] (see Table S2 of the Supporting Information), obtaining the same conclusions.
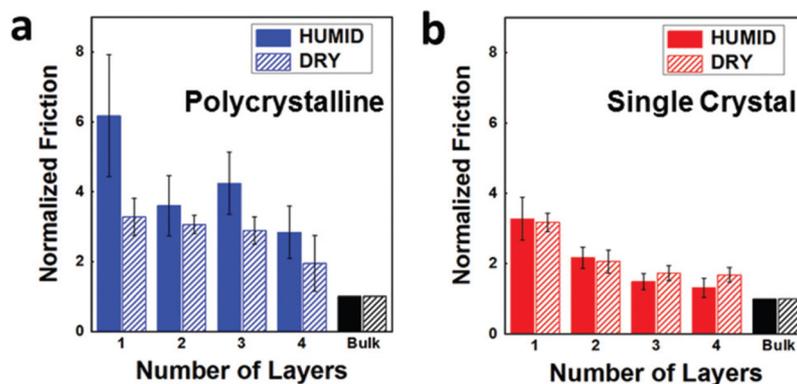

Fig. 3 Comparison of friction forces under humid and dry conditions.

To further explore the origin of the frictional behavior of polycrystalline MoS_2, we perform FFM friction experiments under dry conditions (RH ≈ 5%) (see Fig. 3). Under dry conditions, the oscillatory friction behavior disappears and polycrystalline MoS_2 behaves as the single crystal sample, showing a monotonic decaying trend of F_F *vs.* the number of layers, as can be seen comparing Fig. 3a and b. We conclude that a humid environment is crucial in sustaining the new and very interesting oscillatory behavior observed in polycrystalline MoS2 for an even or odd number of atomic layers.

Here, we propose that the friction oscillatory behavior is related to the odd numbered layers' in-plane piezoelectricity that has been previously demonstrated in MoS_2 single crystal flakes.[21,22] Indeed, because of its crystal structure, MoS_2 shows a broken inversion symmetry when the film presents an odd number of layers, e.g. 1 and 3, with an associated net in-plane permanent polarization (see Fig. 1b);[21] while no piezoelectricity is measured for the symmetric even layers, here 2 and 4 layers (Fig. 1c). For single crystal MoS_2, the in-plane net permanent polarization produces uncompensated electric fields and local charges only at the flake's edges, and not all over the flake's surface, therefore these charges do not impact the friction interactions between the tip and the surface. However, in the case of a polycrystalline film, each odd numbered nanocrystalline grain (∼100 nm in size) of the continuous film displays an in-plane dipole, having a random direction, giving rise to uncompensated electric fields at the grain boundaries which attract charges and adsorbed molecules (see the sketch in Fig. 1g). The humid environment is a source of these charges and charged molecules, such as OH−, while under dry conditions the water concentration drops largely, together with that of such particles.[38] During a friction experiment, when the AFM tip slides on the surface of a polycrystalline odd layer number MoS_2 film, the displacement of these charged molecules on the surface gives rise to an enhanced dissipation and larger frictional forces in odd layer-number films. Friction at the micro- and nanoscale is dominated by short-range interactions between the sliding tip and the surface. Thus, being an energy-dissipating process, it strongly depends on the potential energy landscape of the tip–surface interactions.[24,25]

Several studies show examples of the key role of charges and electronic dissipation in sliding friction.[26,27] Therefore, we can observe a larger friction for polycrystalline samples with an odd

number of layers, compared to the case of samples with an even number of layers, where the absence of polar grains causes a small amount of charged molecules to be absorbed on the surface.

Finally, the high density of GB in polycrystalline samples[39] (see the AFM images in Fig. 1a and 2a (inset)) compared to the monocrystalline case (Fig. 2c (inset)) may explain the overall higher value of friction forces generally recorded in the case of all polycrystalline samples compared to single crystals. GB are generally a source of defects,[40] and thus represent preferential sites for the localization of adsorbates from the environment in all the polycrystalline samples,[41] which as previously discussed increase the friction forces. Accordingly, once in a dry environment, the normalized friction in polycrystalline samples becomes comparable to that of single crystals, confirming the predominant effect of adsorbed charges/molecules at the grain boundaries on friction dissipation.

Since it is well known that the presence of local charges and adsorbed molecules can dramatically change the work function of thin films and 2D materials,[34,42–45] to corroborate our picture we perform XPS and KPFM measurements and analyze the variations in the valence band maximum (VBM) and in the work function (WF) with the number of layers, for both single crystal and polycrystalline MoS_2 samples. We recall that an upward shift in the Fermi energy corresponds to a decrease in the work function and a corresponding increase in VBM.
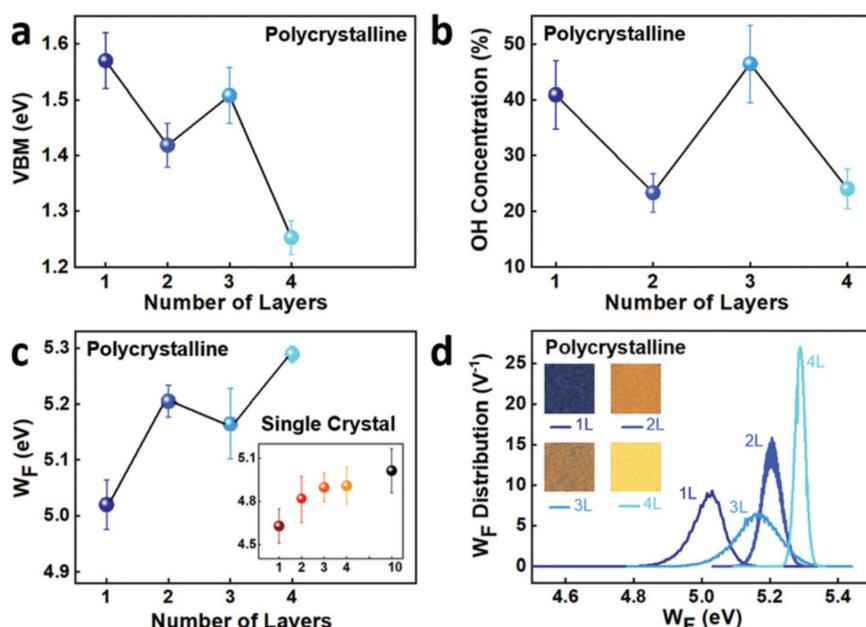

Fig. 4 XPS and Kelvin probe force microscopy of polycrystalline MoS2.

Fig. 4a shows the position of the VBM,[46] measured with respect to the Fermi energy (E_F), as a function of the number of layers in the polycrystalline MoS_2. VBM are extracted from the Mo $4dz^2$ band spectra in the XPS measurements (see Fig. S4 of the Supporting Information). Previous VBM[40,41] and KPFM[33,47,48] measurements on MoS_2 as a function of film thickness showed that the work function of MoS_2 increases with increasing film thickness for two possible reasons. One reason is related to a competing effect between the hole-dopants at the substrate interface[32] and the hole doping molecules adsorbed at the surface, which tend to increase with the thickness due to the screening effect.

A second effect is related to the presence of negatively charged surface states, which generate an electric field between the surface and substrate amplified for thinner films.[40]

Consistently, in our experiments we observe an overall increase of the work function (W_F) with the number of layers for both single crystal and polycrystalline MoS_2 samples (see Fig. 4c and inset), and

a complementary decrease of the VBM in polycrystalline MoS_2 (Fig. 4a). Furthermore, as for the case of friction, in polycrystalline MoS_2 samples we observe an oscillatory behavior related to an odd/even number of layers super-imposed to the monotonic increase of W_F (decrease of VBM).

In particular, the W_F as measured by KPFM is lower for 1L and 3L samples and follows the order $W_F^{1L} < W_F^{3L} < W_F^{2L} < W_F^{4L}$. From our experiments, $W_F^{1L} = 5.01$ eV, $W_F^{2L} = 5.16$ eV, $W_F^{3L} = 5.20$ eV, and $W_F^{4L} = 5.29$ eV (Fig. 4c). The average value and the standard deviation of the work function are obtained from distribution histograms extracted from KPFM images collected on polycrystalline MoS_2 with different numbers of layers (see Fig. 4d and Fig. S7 of the Supporting Information). Accordingly, an upward shift in VBM of a few tenths of electron volts is in fact observed in odd layers (1L and 3L). From Fig. 4a, we observe that 1L and 3L films show higher VBM values (~1.58 eV and ~1.5 eV, respectively) compared to 2L and 4L films (~1.42 eV and ~1.24 eV, respectively). A similar trend is observed also in the Mo 3d and S 2p core level spectra (see Fig. S4 of the Supporting Information). Both core levels show the same oscillating shifts, with 1L and 3L samples having higher binding energies compared to 2L and 4L. This indicates that the whole XPS spectrum undergoes a rigid shift.[41] Since the binding energies of core levels detected in XPS are referred to as the Fermi level of the system, the same observed energy shift can be attributed to a shift in the Fermi energy position, in agreement with the results obtained for the VBM and work function. We attribute the high-energy shift in the core levels of polycrystalline MoS_2 for 1L and 3L to an increased amount of negative charges on the surface.[41] Negative charges could be present in the form of quasi-free electrons, originating from S vacancies at the surface or adsorbed OH ions[47] localized at the grain boundaries of each piezoelectric grain as illustrated in Fig. 1g. Both S vacancies and OH molecules are known to increase the n-doping (or decrease the p-doping) character of MoS_2.[49–52] Elemental analysis obtained from XPS corroborates this hypothesis, showing an increased amount of hydroxyl OH groups in 1L and 3L polycrystalline MoS_2, as shown in Fig. 4b (see also Fig. S5 of the Supporting Information). Furthermore, we find that the S/Mo ratio for all the polycrystalline samples, as determined from Mo 3d and S 2p core level spectra, is higher than 2 (see Fig. S6d of the Supporting Information), making unlikely the presence of sulfur vacancies in these samples.[33,53] Therefore, our results indicate that OH adsorption is the main responsible for the lower p-doping (higher n-doping) character and the corresponding lower work function of polycrystalline MoS_2 with an odd number of layers.

For single crystal MoS_2, VBM data are not available, due to the large XPS beam size which cannot resolve single crystals with only one population of thicknesses (further explanation is reported in the XPS Experimental section and in the Supporting Information). However, nanoscale KPFM experiments show that W_F monotonically increases with the number of layers, from 4.47 eV for 1L MoS_2 to 5.01 eV for a thick 10L crystal (thickness: 6.5 nm), as shown in the inset of Fig. 4c (the corresponding AFM images are shown in Fig. S8 of the Supporting Information). These values are consistent with literature data on MoS_2 single crystals of micrometric size grown by CVD on SiO_2 [48] (see Fig. S8 of the Supporting Information).

As shown in Fig. 4c, polycrystalline samples exhibit a W_F which is 0.3–0.4 V higher than the monocrystalline counterpart, and even higher than bulk MoS_2 (5.2 eV),[54] indicating a more p-doping character. An explanation for the measured higher values of W_F may come from the stoichiometry of the polycrystalline samples, which contain S excess or Mo vacancies in a higher amount compared to the single crystals (see Fig. S4d of the Supporting Information), which are both sources of p-doping.

Accordingly, XPS Mo 3d and S 2p core level spectra resulting from the contributions of single crystals with different thicknesses show an overall blue shift (shift towards higher energies) of the

binding energies when compared to the polycrystalline MoS_2 films having thicknesses between 1 and 4L, see Fig. S4 in the Supporting Information.

Overall, the KPFM and XPS results indicate that the nanograin-associated dipoles emerging in the odd-numbered layer samples attract negatively charged or electron donor molecules at the grain boundaries, in particular OH−, giving rise to the observed larger dissipation in 1L and 3L during the frictional measurements and to a lower W_F and larger VBM for 1 and 3L.

Here, the different dipole orientation in the grains affects the charge distribution[55] and reflects in the width of the W_F histograms from KPFM, which is higher for 1L and 3L compared to 2L and 4L samples (see Fig. 4d).

CONCLUSIONS

In conclusion, our study shows a surprising behavior of polycrystalline continuous films of MoS_2, where friction and work function follow an oscillatory variation for an odd (high friction, low work function) and even (low friction, high work function) number of layers. These phenomena find explanation in the crystalline structure of MoS_2. For polycrystalline MoS_2 films with an odd number of layers, the broken inversion symmetry gives rise to a permanent dipole in each crystalline nano-grain. The KPFM and XPS results indicate that the nanograin-associated dipoles emerging in the odd layer samples attract polar and charged molecules at the grain boundaries. These surface charges change the potential and the sliding energy landscape during tip scanning, giving rise to a larger dissipation in 1L and 3L during the frictional measurements under humid conditions. The same effect is negligible in single crystal MoS_2 structures, where charges are present only at the edges of the large micron-size crystals. Furthermore, being related to the presence of grains in the polycrystalline film structure, we can confidently claim that our observations represent an intrinsic property of polycrystalline MoS_2 2D layers, rather than being limited to the samples analyzed in this study. Understanding the relationship between friction, charges, and atomic structure may help implementing MEMS devices based on MoS_2, whose use in FETs has already been demonstrated. For example, our study suggests that to reduce adhesion in MoS_2 films it would be appropriate to either use an even number of layers or to treat polycrystalline samples with poling, in order to align electric dipoles. Furthermore, this work indicates how local permanent dipoles may affect the work function of 2D materials, which is one of the key properties for the design of electronic devices based on these materials. Finally, it would be possible to extend these findings to other 2D polycrystalline materials which show a similar non center-symmetric structure, like WSe_2.

ACKNOWLEDGEMENTS

REFERENCES

1] H. S. S. Ramakrishna Matte, A. Gomathi, A. K. Manna, D. J. Late, R. Datta, S. K. Pati, et al., MoS_2 and WS_2 Analogues of Graphene, Angew. Chem., Int. Ed., 2010, 49, 4059–4062.

2] J. Y. Park, S. Kwon and J. H. Kim, Nanomechanical and Charge Transport Properties of Two-Dimensional Atomic Sheets, Adv. Mater. Interfaces, 2014, 1, 1300089.

3] C. Berger, Z. Song, X. Li, X. Wu, N. Brown, C. Naud, et al., Electronic Confinement and Coherence in Patterned Epitaxial Graphene, Science, 2006, 312, 1191–1196.

4] S. Kim, S. Zhou, Y. Hu, M. Acik, Y. J. Chabal, C. Berger, et al., Room-Temperature Metastability of Multilayer Graphene Oxide Films, Nat. Mater., 2012, 11, 544–549.

5] Q. Yue, Z. Z. Shao, S. L. Chang and J. B. Li, Adsorption of gas molecules on monolayer MoS_2 and effect of applied electric field, Nanoscale Res. Lett., 2013, 8, 425.

6] A. Castellanos-Gomez, M. Poot, G. A. Steele, H. S. J. van der Zant, N. Agraït and G. Rubio-Bollinger, Mechanical Properties of Freely Suspended Semiconducting Graphenelike Layers based on MoS2, Nanoscale Res. Lett., 2012, 7, 233.

7] H.-J. Jin, W. Y. Yoon and W. Jo, Virtual out-of-plane piezoelectric response in MoS_2 layers controlled by ferroelectric polarization, ACS Appl. Mater. Interfaces, 2017, 10(10), 1334–1339.

8] Y. Zhu, S. Murali, M. D. Stoller, A. Velamakanni, R. D. Piner and R. S. Ruoff, Microwave Assisted Exfoliation and Reduction of Graphite Oxide for Ultracapacitors, Carbon, 2010, 48, 2106–2122.

9] X. Wang, L. Zhi and K. Müllen, Transparent, conductive graphene electrodes for dye-sensitized solar cells, Nano Lett., 2008, 8(1), 323–327.

10] G. H. Lee, Y. J. Yu, X. Cui, N. Petrone, C. H. Lee, M. S. Choi, et al., Flexible and Transparent MoS_2 Field-Effect Transistors on Hexagonal Boron Nitride-Graphene Heterostructures, ACS Nano, 2013, 7, 7931–7936.

11] A. Niguès, A. Siria, P. Vincent, P. Poncharal and L. Bocquet, Ultrahigh Interlayer Friction in Multiwalled Boron Nitride Nanotubes, Nat. Mater., 2014, 13, 688–693.

12] S. Kawai, A. Benassi, E. Gnecco, H. Söde, R. Pawlak, X. Feng, et al., Superlubricity of Graphene Nanoribbons on Gold Surfaces, Science, 2016, 351, 957–961.

13] C. Lee, Q. Li, W. Kalb, X.-Z. Liu, H. Berger, R. W. Carpick, et al., Frictional characteristics of atomically thin sheets, Science, 2010, 328(5974), 76–80.

14] J. S. Choi, J.-S. Kim, I.-S. Byun, D. H. Lee, M. J. Lee, B. H. Park, et al., Friction Anisotropy–Driven Domain Imaging on Exfoliated Monolayer Graphene, Science, 2011, 333, 607–610.

15] A. Klemenz, L. Pastewka, S. G. Balakrishna, A. Caron, R. Bennewitz and M. Moseler, Atomic Scale Mechanisms of Friction Reduction and Wear Protection by Graphene, Nano Lett., 2014, 14, 7145–7152.

16] T. Filleter, J. L. McChesney, A. Bostwick, E. Rotenberg, K. V. Emtsev, T. Seyller, et al., Friction and Dissipation in Epitaxial Graphene Films, Phys. Rev. Lett., 2009, 102, 086102.

17] P. E. Sheehan and C. M. Lieber, Friction between van der Waals Solids during Lattice Directed Sliding, Nano Lett., 2017, 17, 4116–4121.

18] M. Lucas, X. Zhang, I. Palaci, C. Klinke, E. Tosatti and E. Riedo, Hindered Rolling and Friction Anisotropy in Supported Carbon Nanotubes, Nat. Mater., 2009, 8, 876–881.

19] J. Cumings and A. Zettl, Low-Friction Nanoscale Linear Bearing Realized from Multiwall Carbon Nanotubes, Science, 2000, 289(5479), 602–604.

20] M. Chhowalla and G. A. J. Amaratunga, Thin Films of Fullerene-like MoS_2 Nanoparticles with ultra-low Friction and Wear, Nature, 2000, 407, 164–167.

21] H. Zhu, Y. Wang, J. Xiao, M. Liu, S. Xiong, Z. J. Wong, et al., Observation of Piezoelectricity in Free-standing Monolayer MoS2, Nat. Nanotechnol., 2015, 10, 151–155.

22] W. Wu, L. Wang, Y. Li, F. Zhang, L. Lin, S. Niu, et al., Piezoelectricity of single-atomic-layer MoS_2 for energy conversion and piezotronics, Nature, 2014, 514(7523), 470–474.

23] S. Wachter, D. K. Polyushkin, O. Bethge and T. Mueller, A Microprocessor Based on a Two-Dimensional Semiconductor, Nat. Commun., 2017, 8, 14948.

24] I. Leven, D. Krepel, O. Shemesh and O. Hod, Robust Superlubricity in Graphene/h-BN Heterojunctions, J. Phys. Chem. Lett., 2013, 4, 115–120.

25] A. Blumberg, U. Keshet, I. Zaltsman and O. Hod, Interlayer Registry to Determine the Sliding Potential of Layered Metal Dichalcogenides: The Case of 2H-MoS_2, J. Phys. Chem. Lett., 2012, 3, 1936–1940.

26] J. Y. Park, D. F. Ogletree, P. A. Thiel and M. Salmeron, Electronic Control of Friction in Silicon pn Junctions, Science, 2006, 313, 186.

27] T. A. L. Burgo, C. A. Silva, L. B. S. Balestrin and F. Galembeck, Friction Coefficient Dependence on Electrostatic Tribocharging, Sci. Rep., 2013, 3, 2384.

28] M.-Y. Li, Y. Shi, C.-C. Cheng, L.-S. Lu, Y.-C. Lin, H.-L. Tang, et al., Epitaxial Growth of a Monolayer WSe_2-MoS_2 lateral p-n junction with an Atomically Sharp Interface, Science, 2015, 349, 524–528.

29] N. Perea-López, Z. Lin, N. R. Pradhan, A. Iñiguez-Rábago, A. L. Elías, A. McCreary, et al., CVD-Grown Monolayered MoS_2 as an Effective Photosensor Operating at Low-Voltage, 2D Mater., 2014, 1, 011004.

30] A. M. van der Zande, P. Y. Huang, D. A. Chenet, T. C. Berkelbach, Y. M. You, G. H. Lee, et al., Grains and Grain Boundaries in Highly Crystalline Monolayer Molybdenum Disulphide, Nat. Mater., 2013, 12, 554–561.

31] H.-J. Butt and M. Jaschke, Calculation of Thermal Noise in Atomic Force Microscopy, Nanotechnology, 1995, 6, 1–7.

32] W. Liu, K. Bonin and M. Guthold, Easy and Direct Method for Calibrating Atomic Force Microscopy Lateral Force Measurements, Rev. Sci. Instrum., 2007, 78, 063707.

33] J. H. Kim, J. Lee, J. H. Kim, C. Hwang, C. Lee and J. Y. Park, Work Function Variation of MoS_2 Atomic Layers Grown with Chemical Vapor Deposition: The Effects of Thickness and the Adsorption of Water/Oxygen Molecules, Appl. Phys. Lett., 2015, 106, 251606.

34] A. Kahn, Fermi level, work function and vacuum level, Mater. Horiz., 2016, 3, 7–10.

35] E. Riedo, F. Lévy and H. Brune, Kinetics of Capillary Condensation in Nanoscopic Sliding Friction, Phys. Rev. Lett., 2002, 88, 185505.

36] J. Gavoille and J. Takadoum, Surface Charges and Adhesion Measured by Atomic Force Microscope Influence on Friction Force, Tribol. Int., 2003, 36, 865–871.

37] E. Riedo, I. Pallaci, C. Boragno and H. Brune, The 2/3 power law dependence of capillary force on normal load in nanoscopic friction, J. Phys. Chem. B, 2004, 108(17), 5324–5328.

38] Q. Dai, J. Hu and M. Salmeron, Adsorption of Water on NaCl (100) Surfaces: Role of Atomic Steps, J. Phys. Chem. B, 1997, 101, 1994–1998.

39] Z. Ye, A. Balkanci, A. Martini and M. Z. Baykara, Effect of Roughness on the Layer-Dependent Friction of Few-Layer Graphene, Phys. Rev. B, 2017, 96, 115401.

40] W. Jin, P.-C. Yeh, N. Zaki, D. Zhang, J. T. Sadowski, A. Al-Mahboob, et al., Direct Measurement of the Thickness-Dependent Electronic Band Structure of MoS_2 Using Angle-Resolved Photoemission Spectroscopy, Phys. Rev. Lett., 2013, 111, 106801.

41] Y.-K. Lin, R.-S. Chen, T.-C. Chou, Y.-H. Lee, Y.-F. Chen, K.-H. Chen, et al., Thickness-Dependent Binding Energy Shift in Few-Layer MoS_2 Grown by Chemical Vapor Deposition, ACS Appl. Mater. Interfaces, 2016, 8(34), 22637–22646.

42] V. Palermo, G. Ridolfi, A. M. Talarico, L. Favaretto, G. Barbarella, N. Camaioni, et al., A Kelvin Probe Force Mic Charges in All-Thiophene Photovoltaic Blends, Adv. Funct. Mater., 2007, 17, 472–478.

43] O. Ochedowski, B. K. Bussmann and M. Schleberger, Graphene on Mica - Intercalated Water Trapped for Life, Sci. Rep., 2014, 4, 6003.

44] S. Y. Lee, U. J. Kim, J. Chung, H. Nam, H. Y. Jeong, G. H. Han, et al., Large Work Function Modulation of Monolayer MoS_2 by Ambient Gases, ACS Nano, 2016, 10, 6100–6107.

45] O. Ochedowski, K. Marinov, N. Scheuschner, A. Poloczek, B. K. Bussmann, J. Maultzsch, et al., Effect of Contaminations and Surface Preparation on the Work Function of Single Layer MoS_2, Beilstein J. Nanotechnol., 2014, 5, 291–297.

46] E. Kraut, R. Grant, J. Waldrop and S. Kowalczyk, Precise Determination of the Valence-Band Edge in X-Ray Photoemission Spectra: Application to Measurement of Semiconductor Interface Potentials, Phys. Rev. Lett., 1980, 44, 1620.

47] S. Choi, Z. Shaolin and W. Yang, Layer-Number-Dependent Work Function of MoS_2 Nanoflakes, J. Korean Phys. Soc., 2014, 64, 1550–1555.

48] V. Kaushik, D. Varandani and B. R. Metha, Nanoscale Mapping of Layer-Dependent Surface Potential and Junction Properties of CVD-Grown MoS_2 Domains, J. Phys. Chem. C, 2015, 119, 20136–20142.

49] H. Qiu, T. Xu, Z. Wang, W. Ren, H. Nan, Z. Ni, et al., Hopping Transport through Defect-induced Localized States in Molybdenum Disulphide, Nat. Commun., 2013, 4, 2642.

50] C. J. L. de la Rosa, A. Nourbakhsh, M. Heyne, I. Asselberghs, C. Huyghebaert, I. Radu, et al., Highly Efficient and Stable MoS2 FETs with Reversible n-Doping Using a Dehydrated Poly (vinyl-alcohol) Coating, Nanoscale, 2017, 9, 258–265.

51] H.-Y. Park, M.-H. Lim, J. Jeon, G. Yoo, D.-H. Kang, S. K. Jang, et al. Wide-range controllable n-doping of molybdenum disulfide (MoS2) through thermal and optical activation, ACS Nano, 2015, 9(3), 2368–2376.

52] C.-P. L. Lu, G. Li, J. Mao, L.-M. Wang and E. Y. Andrei, Bandgap, Mid-Gap States, and Gating Effects in MoS_2, Nano Lett., 2014, 14, 4628–4633.

53] S. McDonnell, R. Addou, C. Buie, R. M. Wallace and C. L. Hinkle, Defect-Dominated Doping and Contact Resistance in MoS_2, ACS Nano, 2014, 8, 2880–2888.

54] J. Kim, S. Byun, A. J. Smith, J. Yu and J. Huang, Enhanced Electrocatalytic Properties of Transition-Metal Dichalcogenides Sheets by Spontaneous Gold Nanoparticle Decoration, J. Phys. Chem. Lett., 2013, 4, 1227–1232.

55] S. Sadewasser, T. Glatzel, M. Rusu, A. Jäger-Waldau and M. C. Lux-Steiner, High-Resolution Work Function Imaging of Single Grains of Semiconductor Surfaces, Appl. Phys. Lett., 2002, 80, 2979–2981.